

It has been reproduced from the best available copy to permit the broadest possible availability.

ANL-HEP-CP--84-79

DE85 005011

CONF-841007-49

The submitted manuscript has been authored by a contractor of the U.S. Government under contract No. W-31-109-ENG-38. Accordingly, the U.S. Government retains a nonexclusive, royalty-free license to publish or reproduce the published form of this contribution, or allow others to do so, for U.S. Government purposes.

CONSTRUCTION AND OPERATION OF A DRIFT-COLLECTION CALORIMETER

I. Anbats, D. S. Ayres, J. W. Dawson, J. H. Hoftiezer, W. A. Mann, E. N. May, N. M. Pearson,
L. E. Price, K. Sivaprasad, N. Solomey, and J. L. Thron
Argonne National Laboratory, Argonne, IL 60439
and
T. H. Joyce
University of Minnesota, Minneapolis, MN 55455

Introduction

Large area planar drift chambers with long drift distances (up to 50 cm) have been developed for possible use in the new Soudan 2 nucleon decay detector. Design goals included fine sampling to determine the topology of complex events with several low-energy tracks. The large scale of the experiment (> 1000 metric tons) required large area, inexpensive chambers, which also had good position resolution and multi-track separation. The chambers were to be installed between thin sheets of steel to form a fine-grained detector. A second goal was the sampling of dE/dx with each position measurement, in order to determine the direction and particle identity of each track. In this paper we report on the construction and operation of a prototype detector consisting of 50 chambers, separated by 3 mm-thick steel plates. Readout of drift time and pulse height from anode wires and an orthogonal grid of bussed cathode pads utilized 6-bit flash ADC's.

This application of the drift-collection calorimeter technique to a nucleon decay detector¹ follows the investigation by a number of groups²⁻⁴ of calorimeters for high energy detectors based on long drifting.

Construction

The chamber design emphasized compatibility with mass production techniques in order to minimize costs. Their construction is illustrated in Fig. 1. The active area of the prototype chambers is 1 m by 0.5 m, but much longer chambers could be made for a full-sized detector. G10 and copper printed circuit boards 1.6 mm thick form both the cover and gas seal for the chambers and also the electrodes which apply the drift electric field. The covers are separated and the chamber made rigid by a frame made of 1 cm square G10

bars, which surrounds the sensitive region of the chamber and has cross members which divide the sensitive area into two 50 cm squares.

Ionization electrons produced by charged particles traversing the 1 cm thick chamber drift along the 50 cm dimension of the chamber, perpendicular to the drift field electrodes, up to a maximum distance of 50 cm. At the end of the drift region, the electrons are detected by a 1 m long proportional wire (diameter 38 μ m) which is centered between the two cover sheets and 0.5 cm from the edge frame member. Above and below the wire, the copper on the printed circuit boards is segmented into 1.8 cm wide cathode pads on 2 cm centers, in order to read out the coordinate along the wire.

The drift field is produced by 2 mm wide copper lines on the cover plates, spaced 1 cm apart. These drift electrodes are connected through card edge connectors to an external resistor chain which grades the applied drift voltage. In order to control the potential everywhere on the boundary of the drift region, these drift electrodes and the G10 surfaces between them are covered by high resistivity ($\sim 10^{10}$ ohms/square) conducting ink.⁵ The ink is an epoxy-based material which was applied by silk-screening and cured by baking. The inside surfaces of the frame members are also covered by the resistive ink, with the same 10^{10} ohms/square on the frame cross members, which cross the drift electrodes. Lower resistivity (10^6 ohms/square) material is used on the long frame members, which are in contact with the cathode pads or the highest-voltage drift electrode, and are therefore at constant potential.

Bonding of the cover plates to the frame was accomplished with a heat curing epoxy tape.⁶ Since both the epoxy tape and the conducting epoxy ink were cured by similar baking cycles, it was found possible

Cut-away Drift Chamber Schematic

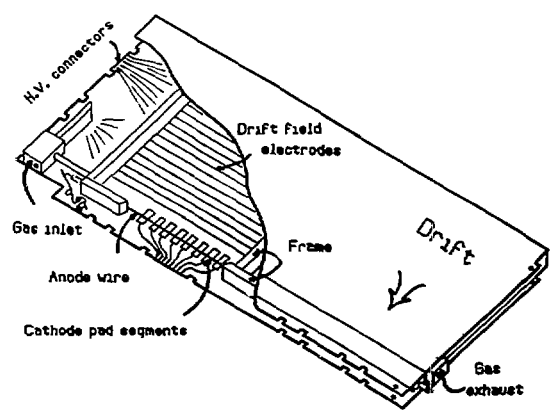


Fig. 1. Cutaway drawing of the long-drifting planar chambers. For clarity, a reduced number of drift field electrodes (there are 48) and cathode pads (there are 25 in each 50 cm length) are drawn.

MASTER

DISTRIBUTION OF THIS DOCUMENT IS UNLIMITED

to assemble the chamber with both the conducting ink and the epoxy tape uncured, and then to cure both in one oven cycle. The chamber components were held flat and under pressure in an assembly fixture. Alignment pins in the fixture assured the precise positioning ($\pm 125 \mu\text{m}$) of the electrodes on each cover relative to one another, in order that there was no component of the drift field into the covers.

Operation

Since the drifting path is relatively long (up to 50 cm) and in a confined space of poor aspect ratio, special care is needed to minimize losses of the drifting electrons. In order to reduce the loss of electrons by diffusion into the walls, we chose a cool gas: 90% argon, 10% CO_2 . The oxygen concentration in the gas was monitored and kept at less than 10 ppm. Higher concentrations produced noticeable attenuation at long drift distances.

The conducting ink interpolates between the potentials of the copper strips, eliminates fields from charged dielectric surfaces, and shields the drift volume from the effects of external conductors. We have further reduced the effects of imperfections in the electric field, and also of diffusion, by use of a focussing electric field:

$$E = E_0 \exp(-bz), \text{ with}$$

$$b = 0.03/\text{cm},$$

where the $+z$ direction is taken opposite to the electron drift direction. The applied drift potential is -10 kV , giving a drift field of 366 v/cm near the anode wire, and 80 v/cm at the longest drift distance. This variation of the z component of the drift field produces a focussing component such that the electron drift direction at the cover plates is pointed toward the center by 16 mrad . The total time for 50 cm drift is $46 \mu\text{sec}$.

The proportional wire was operated typically at $+1750 \text{ volts}$, which produced a gas gain of about 5×10^4 .

Prototype Detector Array

A prototype calorimeter was assembled from 50 drift chambers interleaved with 3 mm thick steel sheets, as shown in Fig. 2. The performance of the device was studied in a low-energy charged particle test beam. The support structure for the 0.6-ton array allowed it to be tipped and rotated such that a wide range of incident angles could be studied. The chambers were connected to a common drift high voltage divider bus, and were supplied in parallel from a single flow-through gas system. A scintillator trigger was provided for cosmic ray studies, as shown in Fig. 2.

Electronics and Readout

An orthogonal two-dimensional readout was obtained from the prototype array by reading out individually each anode wire, bussing corresponding cathode pads from chamber to chamber, and reading out each of the cathode busses. Thus the data from the 50 anode wires gave horizontal track positions and data from the 50 cathode busses gave the vertical positions.

Positive and negative signals from the cathodes and anodes respectively are carried on ribbon bus and coaxial cable to preamplifiers. These are simple common-base-input devices which change the current signal to a voltage output. Twenty meter long AMP 50

Calorimeter Schematic

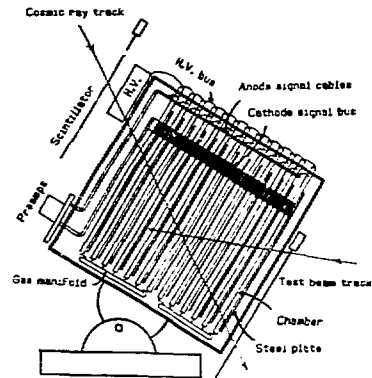


Fig. 2. Prototype calorimeter, 50 drift chambers (fewer are drawn for clarity) were mounted between 3 mm thick steel sheets. Drift and anode high voltages are bussed along the top and cathodes are bussed along the side (only one cathode bus is shown).

mass-terminated ribbon coaxial cables carry these signals to shaping amplifiers with a rise-time of 100 nsec and a fall-time of 480 nsec . The reshaped signal was then presented to the input of a 6-bit flash ADC which digitized the signal amplitude every 150 nsec and stored the result in a random access memory (RAM). The signal shaping to a length greater than the digitization time of the flash ADC allows the original pulse shape to be recovered by a simple linear transformation.

Between triggers and subsequent readout of data, the flash ADC system was constantly digitizing and storing results in a 512 location RAM implemented as a circular buffer. With the 150 nsec clock time for the ADC, 512 locations per readout channel provided a $75 \mu\text{sec}$ window on the time history of the drift chambers. The external trigger, from the coincidence of the two scintillation counters or the test beam electronics, caused the RAM address at the time of the trigger to be stored. The electronics continued digitizing and storing the data for the next $50 \mu\text{sec}$, at which time the clock was stopped and the computer interrupted.

For each channel of readout, 512 data words are recorded. Since only an average of 6-10 of these words are occupied by valid data a special data preprocessor was built to scan the data before transfer to the host computer, deleting those data words with ADC channels below a preset threshold. For each ADC count above threshold, the clock address and data are concatenated and written into a FIFO buffer.

A more complete description of the electronic system is given by Dawson, Hay, and Soloney in these proceedings.

Data Taking

The 50 chamber prototype array was exposed to a beam containing positive and negative pions, muons, and electrons, whose momentum was varied from 150 to 400 MeV/c , a range appropriate to the intended use in the Soudan 2 nucleon decay experiment. The beam was

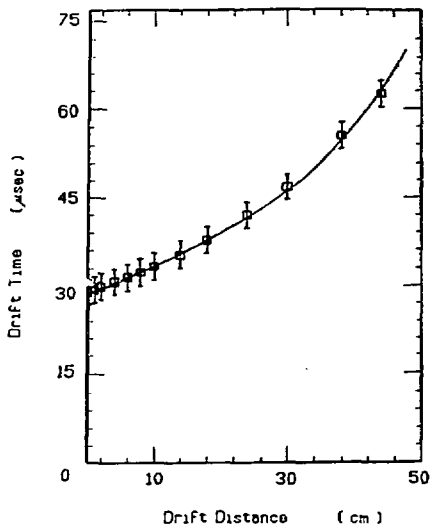


Fig. 3. Drift time vs. drift distance.

produced by the 500 MeV protons of the Argonne National Laboratory Intense Pulsed Neutron Source facility. Each test-beam particle was identified by time-of-flight measurement. In separate runs, the prototype detector readout was triggered on cosmic ray particles, in order to observe tracks traversing all

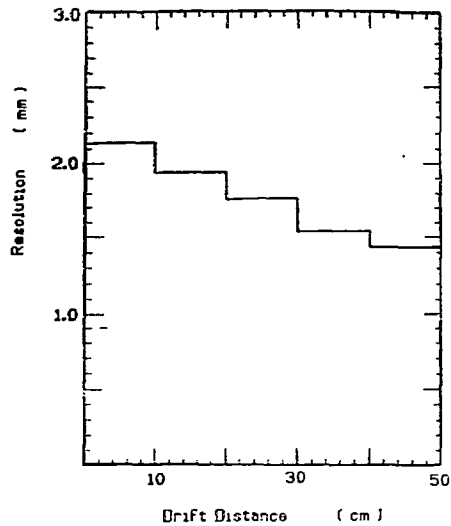


Fig. 4. Position resolution calculated from residuals to straight-line fits to tracks as a function of drift distance.

parts of the drift chambers and determine uniformity of response.

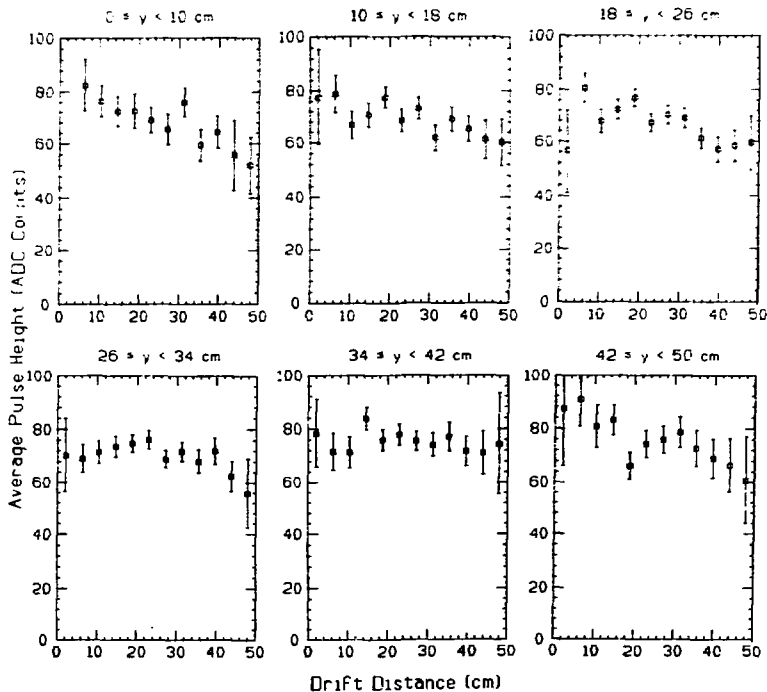


Fig. 5. Response of chamber to cosmic ray tracks vs. position in chamber. Each graph plots the average pulse height vs. the drift distance for the vertical range written above the graph.

Performance of Prototype Detector

The time vs. distance relationship in typical chambers was measured using a scintillator and a radioactive source. The results are plotted in Fig. 3. The varying drift velocity resulting from the exponential field is quite evident. This velocity profile could be expected to lead to a position resolution which improves with increasing drift distance, if the position resolution is dominated by the ADC clock. The position resolution as determined from residuals of track fitting is shown in Fig. 4. The resolution is seen to diminish only slightly from the shortest drift distances to the longest, indicating that the effect of electron diffusion is beginning to dominate at long drift distances.

Cosmic ray tracks have been used to determine the uniformity of response of the chambers over their area. Fig. 5 plots the average pulse height as a function of position over a representative 50 cm

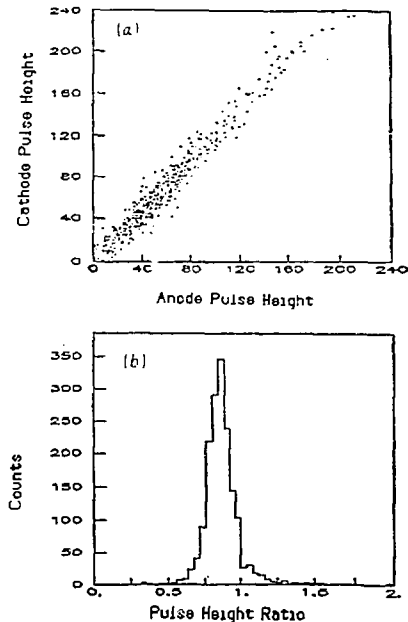


Fig. 6. Anode vs. cathode pulse height correlation. (a) Scatter plot. (b) ratio (anode pulse height)/(cathode pulse height).

square section of one chamber. All vertical sections are consistent with an average attenuation of 23%, giving an electron lifetime of 180 μ sec. Proportionality between anode and cathode signals is shown in Fig. 6, which shows (a) a scatter plot of cathode vs. anode signals and (b) a histogram of the ratio of anode pulse height/cathode pulse height. (Although the raw cathode signal has about one-third the charge of the anode signal, the choice of preamplifier gains has made the amplified cathode signal slightly larger.)

A prime reason for including measurement of dE/dx in a nucleon decay detector is to determine the direction of motion of a particle along a track, so that a decay vertex can be distinguished from the interaction or scattering of a single particle. Since

direction measurement derives from the increase in dE/dx as the particle slows down, we show in Fig. 7 a scatter plot of the sum of the first 5 chamber signals vs. the sum of the last 5 chamber signals for 250 MeV/c stopping muon tracks. The direction is correctly determined if the signal from the last 5 is greater than that from the first 5, i.e. the point in the scatter plot is above the 45° line. In this example, the direction is correctly determined for $87 \pm 1\%$ of the tracks.

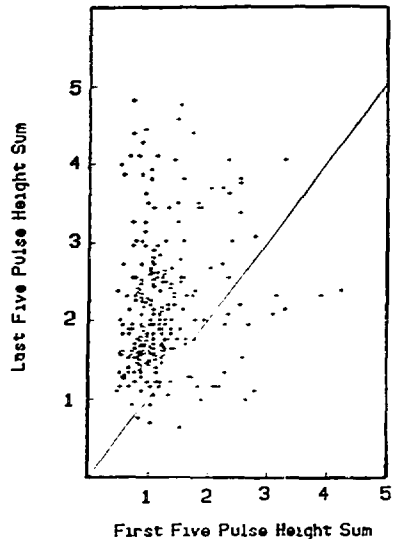


Fig. 7. Use of dE/dx to determine direction of 250 MeV/c muon tracks. See text for details.

Detailed analysis of identified beam track topologies will be discussed elsewhere, but we end this paper with representative event displays of a pion (Fig. 8a), a muon (Fig. 8b) and an electron (Fig. 8c). The figures show the qualitatively different appearance expected in such a fine-grained

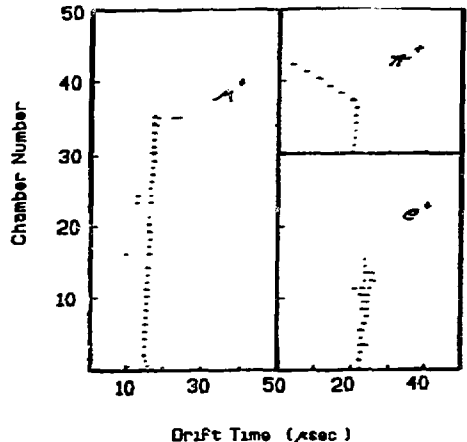


Fig. 8. Examples of μ^+ , π^+ , and e^+ tracks in the prototype detector, showing characteristic differences that allow identification of particle tracks.

tracking detector; the muon is straight except for a small amount of multiple Coulomb scattering as it stops; the pion undergoes a large-angle scatter; and the electron, even at this low energy, shows the ragged appearance of an electromagnetic shower. (Only the anode-wire view is shown for each event. Note that the track display of Fig. 8 shows the pulse-height profile of each drift chamber hit, as it is measured by the flash ADC.

References

1. L. E. Price, et al., IEE Trans. Nucl. Sci. NS-29, 383 (1982).
2. L. E. Price, Proc. Int. Conf. on Instr. for Colliding Beam Physics (SLAC-250), 206 (1982).
3. E. Albrecht et al., SLAC-250, 212 (1982).
4. M. Berggren et al., Nucl. Instr. Meth. 225, 477 (1984).
5. Methode Development Co., Chicago, IL.
6. JM Company, Minneapolis, MN.
7. J. Dawson, E. Hay, and N. Solomey, "Data Preprocessor and Compactor for Soudan 2 Nucleon Decay Experiment", these proceedings.

DISCLAIMER

This report was prepared as an account of work sponsored by an agency of the United States Government. Neither the United States Government nor any agency thereof, nor any of their employees, makes any warranty, express or implied, or assumes any legal liability or responsibility for the accuracy, completeness, or usefulness of any information, apparatus, product, or process disclosed, or represents that its use would not infringe privately owned rights. Reference herein to any specific commercial product, process, or service by trade name, trademark, manufacturer, or otherwise does not necessarily constitute or imply its endorsement, recommendation, or favoring by the United States Government or any agency thereof. The views and opinions of authors expressed herein do not necessarily state or reflect those of the United States Government or any agency thereof.